International Symposium of Research Students on Materials Science and Engineering
December 20-22, 2004, Chennai, India
Department of Metallurgical and Materials Engineering, Indian Institute of Technology Madras

SPARK PLASMA SINTERING OF TiB_2-BASED COMPOSITES

T. Venkateswaran[1], Bikramjit Basu[1] and Doh-Yeon Kim[2]
[1]*Department of Materials and Metallurgical Engineering,*
Indian Institute of Technology, Kanpur, India.
[2]*School of Materials Science and Engineering and*
Centre for Microstructure Science of
Materials, Seoul National University, Seoul 151-744, Korea.

ABSTRACT

The densification of TiB_2 has been a major problem due to strong covalent bonding, low self-diffusion coefficient and the existence of oxygen rich surface layer on the particle surface. The selection of binder (type and amount) and the processing parameters is required to obtain dense borides. In this exploration, the sintering of monolithic TiB_2 and TiB_2 with 10 wt% of $MoSi_2$ addition is carried out using Spark Plasma Sintering (SPS) technique. SPS experiments are carried out in the temperature range of 1300°C to 1500°C for a holding period of 10 min under vacuum. The enhanced sintering of monolithic TiB_2 to full density at lower temperature (1400°C) ensures the grain boundary cleaning and enables binderless sintering in SPS route. Furthermore, the synergetic effect of sintering aid ($MoSi_2$) as well as SPS processing route enhanced the densification of TiB_2 composites at the same temperature of matrix densification in shorter time (10 minutes). The mechanical and electrical properties of the developed TiB_2 composite are also evaluated. Further detailed microstructural analysis of the SPS processed sample is carried out using XRD and SEM in order to understand the detailed densification mechanism.

Keyword: TiB_2, $MoSi_2$, Spark Plasma Sintering

1. INTRODUCTION

The attractive combination of hardness, thermal and electrical properties of TiB_2 based materials made them suitable for various engineering applications, such as cathode material for hall heroult cell, aluminum evaporation boat, Electro Discharge Machining (EDM) electrode, armour material, conductive coating and wear components [1-4]. Because of strong covalent bonding, high melting point and relatively low self-diffusion coefficient, the densification of monolithic Titanium di-boride (TiB_2) is needed to be carried out at relatively high sintering temperature (>1800°C) and longer holding time (> 1h) in conventional pressureless sintering route [5-8]. Moreover, internal stresses as a consequence of grain growth at higher sintering temperature triggers microcracking, resulting in degradation of mechanical properties[9, 10-13].

Alternatively, the use of ceramic binders is also explored in achieving maximum densification with better properties [11, 14-16]. The major motivation behind the addition of binders is to eliminate the oxide layer from the TiB_2 particle surface and results in the formation of amorphous or crystalline phase during sintering. The elimination of oxide layer can be achieved in two ways: a) by addition of sintering additives, b) by high temperature sintering to evaporate oxygen rich species (TiO_2). Various reaction products e.g. SiO_2, $(Ti, Zr)_5Si_3$, $(Ti, Zr)B_2$, $(Ti, Ta)B_2$ are reported to be formed with addition of various sintering additives like SiC, ZrO_2, TaC, TaN respectively to TiB_2 base material [17-19]. Also, another group of researchers used reaction sintering and mechanochemical processing route to obtain TiB_2-based composite with

better densification and mechanical properties [20, 21]. In this investigation, $MoSi_2$ is selected as a sintering additive for TiB_2 material. $MoSi_2$, an intermetallic compound, is a candidate material for high temperature applications and often used as heating elements, aircraft components, turbine blades etc.[22,23] Optimized amount of $MoSi_2$ addition to TiB_2 can potentially lead to the development of particulate reinforced ceramic-ceramic composite with improved thermal and electrical properties for high temperature application. In a recent work, we reported the microstructure and properties of TiB_2-$MoSi_2$ materials, processed via hot pressing route [24]. It was observed that full densification and better mechanical properties can be obtained after hot pressing at 1700°C for 1 h with 10 wt. % $MoSi_2$ addition. Following this, the present work is taken up to investigate the densification and property study using SPS as a processing tool. Now-a-days Spark Plasma Sintering (SPS) is widely used for faster sintering of nanomaterials as well as various structural materials [25-27]. The present investigation will explore the synergetic effect of addition of sinter-additive ($MoSi_2$) and SPS processing route on the densification and properties of TiB_2-based materials.

2. EXPERIMENTAL

2.1 Starting powders and densification

The in-house synthesized TiB_2 and $MoSi_2$ were selected as starting powders. TiB_2 is produced by borothermic reaction among TiO_2 (> 99% purity, Merck, Germany), B_4C (In-house) and C. $MoSi_2$ powders are processed from elemental Mo (> 99% purity, supplier Leco Industries, U.S.A) and Si (>99% purity, supplier Merch, Germany). The mean particle diameter and particle size distribution was measured using laser particle size analyzer (Analysett 22). The specific surface area was measured by BET (COULTER, SA300). Planetary milling of TiB_2 and $MoSi_2$ starting powders in weight ratio of 90:10 was conducted with WC milling balls for 24 hours using acetone as a milling media to obtain mixed powders and to break the agglomerate. The starting particle sizes (D_{50}) of TiB_2 and $MoSi_2$ are 0.5-2 μm and 2-3 μm respectively. Also TiB_2 particles are of spherical shape, whereas $MoSi_2$ particles are of sharply faceted and of irregular shape.

Appropriate weight of premixed powders was placed in a graphite mold of 10 mm internal diameter with proper graphite insulation around it to prevent interaction of powders with graphite mold. The SPS chamber is closed firmly and high vacuum of 70 mtorr is maintained throughout the experiment. DC current of 1- 1.5 kA and DC voltage of 5-10 V are applied and variation in this range depends on the final holding temperature. The experiments are carried out in the temperature range of 1300°C – 1500°C with a heating rate of 500 K/min with holding time of 10 minutes and applied pressure of 40 Mpa.

2.2 Characterization

The density of spark plasma synthesized samples was measured in water following Archimedes principle. Further, phase identification was performed using X-ray diffraction using Cu Kα radiation (Rich-Seifert, 2000 D). The Elastic Modulus (E) was measured using pulse-echo resonance frequency method (Tektronix TDS 200, Panametrics Model 5800). The Vickers Indentation is carried out on well polished surface to measure hardness and toughness at load of 10 kg with a dwelling time of 15 s on a Universal Hardness tester. The Fracture toughness is evaluated by crack length measurement (2a) around the radial crack pattern formed by Vickers indentation adopting formulation proposed by Anstis et al. [28]. Detailed Microstructural investigation of the polished and fractured composites was performed using Scanning Electron Microscopy (FE-SEM, JSM-6330F) Elemental analysis of different phases are examined using EDS equipped with SEM. Electrical resistivity (dc) was measured by standard four probe method at room temperature with appropriate silver epoxy-coating on the flat materials, followed by hardening at 150°C.

3. RESULTS

3.1 Densification

The densification data of the developed TiB_2-based composites and corresponding monolithic (TiB_2 and $MoSi_2$) materials are presented in Fig. 1. The maximum densification of Monolithic TiB_2 (~98% ρ_{th}) and $MoSi_2$ (~95% ρ_{th}) occurs at the SPS temperature of 1400°C. The developed TiB_2 – 10 wt. % $MoSi_2$ composite exhibits maximum densification (~ 98 % ρ_{th}) in the SPS processing temperature of 1400°C for a holding period of 10 min. In general, conventional Pressureless sintering of the TiB_2 based materials are carried out in the temperature range greater than 1800°C and the densification is generally assisted i.e. enhanced with pressure (HIP, HP) [15,29-30]. The present experimental results clearly indicate that SPS synthesis route is attractive in achieving better densification at a temperature 400-500°C lower than other conventional sintering technique.

3.2. Microstructural Characterization

Fig. 2 presents XRD analysis of the TiB_2-10 wt. % $MoSi_2$ composite, SPSed at 1400^0C and 1500^0C, revealing the presence of the various crystalline phases. Beside the predominant presence of TiB_2 and $MoSi_2$, the noticeable presence of $TiSi_2$ could be easily detected. SEM images of the fracture surfaces of the monolithic TiB_2 and $MoSi_2$ are depicted in the Figs. 3a & b. Monolithic TiB_2, with maximum densification (~ 98 % ρ_{th}), is characterized by the presence of the isolated closed pores. Also, the fracture surface of the monolithic TiB_2, SPSed at 1400^0C for 10 min, shows the presence of well faceted equiaxed TiB_2 grains with intercrystalline pores trapped between the grains and also at the triplet junction (Fig. 3a). The microstructure of monolithic TiB_2 material is characterized by the average grain size of 2-5 μm. The observed fracture mode in the monolithic TiB_2 is purely intergranular in nature. Fig. 3b presents the fracture surface topography of SPSed monolithic $MoSi_2$. The fractograph is characterized by disintegration of $MoSi_2$ particles (grey contrast) leading to loss of particle shape. In fact, it is difficult to characterize the microstructure with a specific grain size. Additionally, EDS analysis reveals that the black contrast phase is SiO_2. Observing Fig. 3b also reveals that SiO_2 phase probably has melted during SPS processing. Also, SiO_2 phase is observed to be trapped between $MoSi_2$ particles. Some SiO_2 particles are also present in intercrystalline region. The topographical features implicate that the dominant fracture mode is of transgranular nature.
The formation of SiO_2 can be linked to the 'Pest behavior' of $MoSi_2$. Similar observation was also made for $MoSi_2$ [31,33].Chou at. al. proposed a thermodynamically feasible reaction (favorable upto 3327°C) to explain the pest behavior [32]:

$$MoSi_2\,(s) + 7/2\ O_2\,(g) \rightarrow MoO_3\,(g) + 2SiO_2(l)$$

In the SPS sintering, generation of Spark Plasma results in the vaporization and melting of SiO_2 protective layer on the particle surface. This, in combination with TiO_2 layer of TiB_2 leads to the formation of $TiSi_2$ reaction product. Fig. 3c & d. presents the SEM images of the fracture and polished surfaces of the, SPSed at 1400°C for 10 minutes. The developed composite showing the mixed mode of intergranular and transgranular type of fracture (Fig. 3a). Figs. 3d illustrate the BSE micrographs obtained from the polished surfaces. The microstructure is characterized by the three phases with grey, black and white contrast. EDS analysis of different phases confirms that the grey and white phases are TiB_2 and $MoSi_2$ respectively. While the third phase with black/dark contrast is rich with Ti and Si (see insert of Fig. 3d). This observation along with XRD results confirms that the black phase probably is $TiSi_2$.

3.3. Mechanical and Electrical property

Fig.4 plots of hardness and fracture toughness as a function of SPS temperature. The developed TiB_2-10 wt.% $MoSi_2$ composite exhibits maximum hardness of ~16.5 GPa at sintering temperature of 1500°C and showing an increase in trend with increasing SPS sintering temperature. No significant change in mechanical property at sintering temperature of 1400 and 1500°C is observed. The E-modulus of the developed composite material is around ~390 GPa, which is lower than that of monolithic TiB_2. The fracture toughness of the developed composite varies from 3.9 to 4.5 MPa $m^{1/2}$ and exhibits higher value at the sintering temperature of 1500°C. The monolithic TiB_2, SPSed at 1400°C exhibits hardness of 17.5 GPa and fracture toughness of 4.8 MPa $m^{1/2}$. Also, monolithic $MoSi_2$ exhibits hardness of around 10 GPa and fracture toughness of ~3 MPa $m^{1/2}$. The lowering of the hardness value of the developed TiB_2 based composite material is due to second phase ($MoSi_2$) addition and formation of reaction product ($TiSi_2$), having poor mechanical property. Moreover, observed abnormal grain growth of some TiB_2 grains may also play a role in lowering of the hardness value. Fig. 3d. Illustrates the propagation of the indentation induced crack. Closer look at Fig. 3d reveals that grey harder TiB_2 particles enhances the crack deflection and the black $TiSi_2$ particle allow crack propagation through it by fracturing. The electrical resisitivity of the developed composite material increase with increasing processing temperature i.e increase with increase in densification and showing the maximum of 12.38 μΩ. cm for composite processed at 1500°C. The electrical resistivity of the monolithic TiB_2 and $MoSi_2$ processed at 1400°C are 13.26 μΩ –cm and 18.87 μΩ –cm respectively.

4. DISCUSSION

In this present investigation, the addition of 10 wt. % $MoSi_2$ and plasma assisted sintering provides better densification of the composite material at much lower temperature and sintering time. As far as the densification is concerned, the following issues need to be considered a) role of Spark Plasma sintering in attaining maximum densification in shorter sintering temperature and time. b) Role of second phase addition and reaction product on the densification kinetics. Both the phenomenon are assisted by physical and chemical activation of the powder particle surface and added up to the driving force for the densification. Apart from the covalent bonding and low self-diffusion coefficient, additional difficulty in densification of TiB_2 arises from the presence of the surface oxides e.g. TiO_2 and B_2O_3 on particle surface. Thermodynamically, the evaporation of B_2O_3 is much more feasible before densification begins and in addition little carbon addition or contamination remove its adverse effect [35]. Practically, the removal of TiO_2 requires very high processing temperature and appropriate binder addition. The combination of grain boundary cleaning mechanism contribution from SPS and reaction product formation by the addition of the sintering additives effectively, leads to faster densification of the composite. The evaporation of material during SPS is strongly dependent on atomic weight, density and sintering temperature [36]. For our composite, the evaporation rate of $MoSi_2$ will be larger. Thus the addition of second intermetallic phase ($MoSi_2$) enhances the sintering kinetics and trigger neck growth during densification. The addition of sintering aid result in the formation of the reaction product of $TiSi_2$, which in turn promotes the densification and enhances electrical property of the developed composite material. The thermodynamically feasible reaction leads to the formation reaction product is given as follows,

$$TiB_2 + 3O_2(g) + MoSi_2 \rightarrow TiSi_2 + B_2O_3(g) + MoO_3(g)$$

Moreover from the microstructural observation of the monolithic $MoSi_2$, distinguished by the presence of SiO_2 inclusion, there are some possibilities of providing Si to combine with TiO_2 to form $TiSi_2$ reaction product. The disintegration (lower average grain size and morphology in the SPS processed material) of the $MoSi_2$ in the developed composite microstructure gives more

supporting to the abovementioned possible reaction. In addition fluxing of the surface layers (TiO_2 from TiB_2 and SiO_2 from $MoSi_2$) because of the SPS processing route also added for the justification. The formation of the reaction product provides the active path for the mass transportation during the sintering process. Sade and Peelleg reported the formation of $TiSi_2$ from the TiB_2 containing free Ti and with Si from the substrate as result of annealing above 765°C [37].

5. CONCLUSION

a) For the first time, binderless densification of monolithic TiB_2 to near theoretical density (~98 % ρ_{th}) is achieved by Spark Plasma Sintering at 1400°C for 10 minutes. The obtained material is characterized by 2-5 μm grain size, high hardness of ~18 GPa and moderate indentation toughness of ~ 5 MPa $m^{1/2}$.
b) The addition of 10 % $MoSi_2$ does not seem to improve the sinterability of TiB_2 matrix. Almost fully dense composites are obtained under the same SPS conditions for matrix densification XRD as well as SEM-EDS analysis reveals the formation of $TiSi_2$ phase dispersed in the microstructure. The densification mechanism is dominated by liquid phase sintering in the presence of $TiSi_2$. TiB_2 particles size in the composite varies around 1-3 μm.
c) The improvement of mechanical properties in composite is not considerable as same hardness (~17 GPa) as TiB_2 monolithic is measured. The fracture toughness remains moderate (~ 4.5 MPa $m^{1/2}$) and this is due to the presence of brittle intermetallic phase ($TiSi_2$ and $MoSi_2$).
d) Although, enhancement of mechanical property is not realized as compared to monolithic TiB_2, higher electrical conductivity (0.081-0.092 x 10^6 Ω^{-1} cm^{-1}) is measured with composite. This is presumably due to the presence of $TiSi_2$ reaction product.

Acknowledgement: The use of SPS facility available at Sintering and Microstructure lab, Creative Research Centre, School of Materials Research Centre, School of Material Science, SNU, South Korea is gratefully acknowledged. The author wish to express heartily thanks to the members of Sintering and Microstructure laboratory and Thin film & Microstructure laboratory (TFML) for their nice co-operation and guidance. We are grateful to Dr. A. K. Suri of BARC, Department of Atomic Energy (DAE), Government of India for providing the TiB_2 and $MoSi_2$ powders.

6. REFERENCES

[1] V. J. Tennery, C. B. Finch, C. S. Yust and G. W. Clark, Ed: Viswanadhan et.al. , "Structure-property correlations for TiB_2-based ceramics Densified using active liquid metals", Science of Hard Materials, PP 891-909, Plenum, New York, (1983).
[2] B. Todd, "Energy Reduction in Hall-Heroult Cells with conventional and special electrodes", J. Met., 33 [9] 42-45 (1981).
[3] J. M. L. Wilkins, " Boron and Refractory borides", edited by V. I. Matkovich (Spring-verlag, New York, 633 (1977).
[4] Mroz. C., Titanium diboride, Am. Ceram. Soc. Bull., , 74, 158-159 (1995).
[5] Matkovich, V. I., Boron and Refracotry Borides, Spring, Berlin, 172 (1997).
[6] M. Einarsrud, E. Hagen, G. Petterson and T. Grande, "Pressureless Sintering of Titanium diboride with Nickel, Nickel boribe and iron additives", J. Am. Ceram. Soc., 80 [12] 3013-3020 (1997).
[7] M. K. Feber, P. F. Becher and C. B. Finch, "Effect of microstructure on the properties of the TiB2 ceramics", J. Am. Ceram. Soc., 66 [1] C-2-C-4 (1983).
[8] C. B. Finch, P. F. Becher, P. Angelini, S. Baik, C. E. Banberger and J. Brynestod, "Effect of impurities on the densification of submicormeter TiB_2 powders", Adv. Ceram. Mater, 1 [1] 50-54 (1986).

[9] G. Petzow, R. Telle, New Development in the field of refractory hard metals based on cemented borides in: S. Somiya (Ed.), Advanced Ceramics, Terro Scientific Publishing Company, Tokyo, 131-143 (1987).
[10] Z. T. Zakhariev, M. S. Ivanova, I. Serebriankova, Hard materials based on cemented TiB2-WC-Co alloys, Z. Metalkal. 85 [11] 801-803 (1994).
[11] T. Graziani and A. Bellosi, "Sintering and characterization of TiB_2-B_4C-ZrO_2 composites", Materials and Manufacturing Processes, 9 [4] 767-780 (1994).
[12] S. H. Kang, D. J. Kim, E. S. Kang and S. S. Baek, Pressureless Sintering and Properties of Titanium Diboride Ceramics Containing Chromium and Iron, J. Am. Ceram. Soc., 84 [4] 893-895 (2001).
[13] D. G. Ahn, A. Kawasaki, R. Watanabe, Microstructure and Mechanical properties of TiB_2 –W cermets prepared by HIP, Mater. Trans. JIM 37 [5] 1078-1083 (1996).
[14] S. Torizuka, K. Sato, J. Harada, H. Yamamot and H. Nishio, "Microstructure and sintering mechanism of TiB_2-ZrO_2-SiC composite", J. Ceram. Soc. Japan, 100 [4] 392-397 (1992).
[15] S. Torizuka, K. Sato, H. Nishio and T. Kishi, "Effect of SiC on interfacial reaction and sintering mechanism of TiB_2", J. Am. Ceram. Soc., 78 [6] 1606-1610 (1995).
[16] J. Ho Park, Y. Koh, H. Kim C. Hwang and E. Kong, "Densification and Mechanical Properties of Titanium Diboride with Silicon Nitride as Sintering Aid", J. Am. Ceram. *Soc.,* 82 [11] 3037-3042 (1999).
[17] S.Torizuka and T.Kishi, "Effect of SiC and ZrO_2 on sinterability and mechanical properties of titanium nitride, titanium carbonitride and titanium diboride," Materials Transactions, JIM, 37 [4] 782-787 (1996).
[18] R. Telle, S. Meyer, G. Petzow and E.D. Franz, "Sintering Behavior and Phase Reactions of TiB_2 with ZrO_2 Additives," Materials Science and Engineering *A* 105/106 125-129 (1988).
[19] Y. Murata, H.P. Julien and E.D. Whitney, "Densification and wear resistance of ceramic systems: I. Titanium Diboride," *Ceramic Bulletin*, 46 [7] (1967).
[20] H-Jong Kim, H-J Choi and J-G Lee, Mechanochemical Synthesis and Pressureless Sintering of TiB_2-AlN Composite, J. Am. Ceram., 85 [4] 1022-1024 (2002).
[21] G. Wen, S. B. Li, B.S Zhang and Z. X. Guo, Reaction Synthesis of TiB2-TiC Composites with enhanced toughness. Acta mater. 49 1463-1470 (2001).
[22] A. K. Vasudevan, J. J. Petrovic, A comparative Overview of molybdenum disilicde composites, Mater. Sci. Eng. A 155 1-2 (1992).
[23] A. Costa e Silva and M .J. Kaufman, Mater. Sci. Eng. A 195 [1] 75-88 (1998).
[24] T. S. R. Ch. Murthy, B. Basu, R. Balasubramaniam, A. K. Suri, C. Subramanian and R. K. Fotedar, Processing and properties of Novel TiB_2-based composites (going to communicated).
[25] B. Basu, J. H. Lee and D. Y. Kim, "Development of Nanocrystalline wear resistant Y-TZP ceramics", J. Am. Cer. Soc., 87 [9] 1771-1774 (2004).
[26] S. W. Wang, L. D. Chen and T. Hirai; Densification of Al_2O_3 powder using spark plasma sintering; J. Mat. Res., 15[4] 982 (2000).
[27] J. R. Groza, A. Zavalianges, Sintering Activation by external electric field, Mat. Sci. and Engg., A287 171-177 (2000).
[28] Anstis, G. R., Chantukul, P. Lawn, B.R. and Marshall, D.B., "A critical evalution of indentation techniques for measuring fracture toughness", J. Am. Cer. Soc., 64, 553-557 (1981).
[29] S. Tuffe, J. Dubois, G. Fantozzi and G. Barbier, Densification, Microstructure and Mechanical Properties TiB_2-B_4C Based Composites, Int. J. of Refractory Metals and Hard Materials 14 305-310 (1996).
[30] Wang Yucheng and Fu Zhengyi, Study of temperature field in spark plasma sintering, Materials Science and Engineering B90 34 - 37 (2002).
[31] H. Shimizu, M. Yoshinaka, K. Hirota, O. Yamagunchi, Fabrication and Mechanical properties of monolithic $MoSi_2$ by Spark Plasma Sintering, Mat. Res. Bull, 32 1557-1563 (2002).
[32] Chou TC, Nieh TG, Mechanism of $MoSi_2$ pest during low temperature oxidation, J. Mater. Res. 8 [1] 214 (1993).

[33] Y. Q. Liu, G. Shao, P. Tsakiropoulos, On the Oxidation behaviour of $MoSi_2$, Intermetallics, 9 125-136 (2001).
[34] J W Lee, Z. A. Munir, M. Shibuya and M. Ohyanagi, Synthesis of Dense TiB_2-TiN Nanocrystalline Composites through Mechanical and Field Activation, J. Am. Ceram. Soc., 84 [6] 1209-1216 (2001).
[35] S. Baik and P.F. Becher, "Effect of oxygen contamination on densification of TiB_2," *J. Am. Ceram. Soc*., 70 [8] (1987) 527-30.
[36] R. Holm, Electric contacts: Theory and applications, 4th end Spring, New York, 1967.
[37] G. Sade and J. Pelleg, Co-Sputtered TiB_2 as a diffusion barrier for advanced microelectronics with Cu metallization, Applied Surface Science, 91 263-268 (1995).

FIGURES

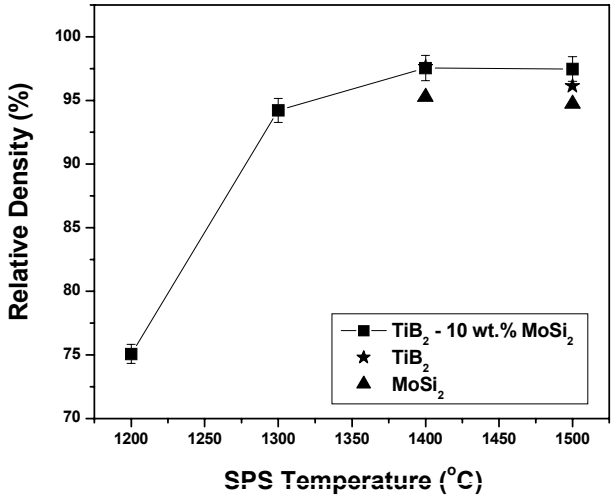

Fig. 1. Plot of relative density versus spark plasma sintering temperature for monolithic TiB_2, TiB_2- 10 wt. % $MoSi_2$ composite and monolithic $MoSi_2$.

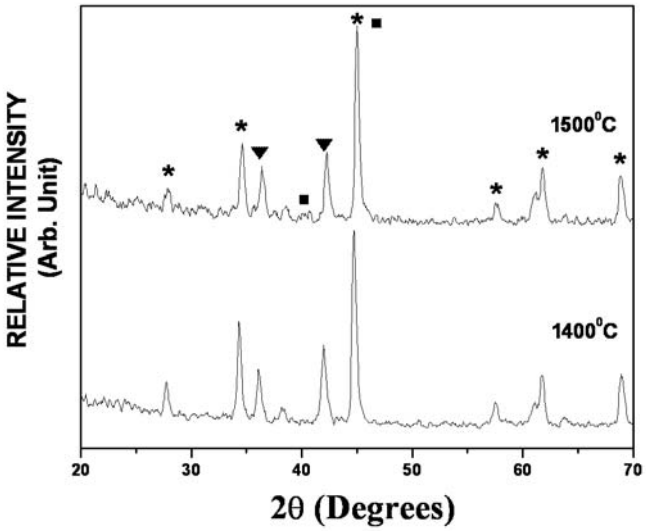

Fig. 2. X-ray diffraction pattern of TiB_2- 10 wt. % $MoSi_2$, SPSed at 1400°C and 1500°C for 10 min under vacuum (c). The different crystalline phases are TiB_2 (*), $MoSi_2$ (■), $TiSi_2$ (▼).

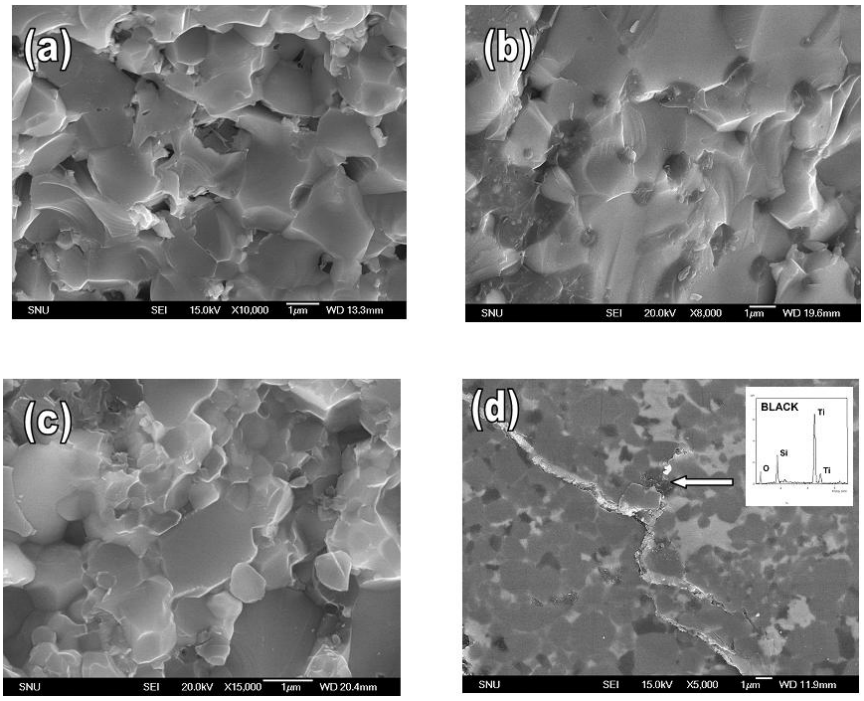

Fig. 3. Scanning electron micrographs of fracture surfaces of monolithic TiB_2 Spark Plasma Sintered at 1400°C for 10 min, showing the presence of intercrystalline pores between grains and triplet junction (a) and monolithic $MoSi_2$, SPS processed at 1400°C for 10 min reveals the presence of SiO_2 inclusion (black) along the grain boundaries, triplet junction (b) Fractography of TiB_2-10 wt. % $MoSi_2$ composite SPS processed at 1500°C for 10 min showing mixed intergranular and transgranular fracture mode (c) and BSE mode of fracture surface of same composite, white contrast on microstructure is $MoSi_2$ (d). SEM images of polished surface revealing three phases: TiB_2(grey), $MoSi_2$(bright) and $TiSi_2$(dark) respectively (c & d). There is an observation of noticeable crack deflection on the developed composite (d).

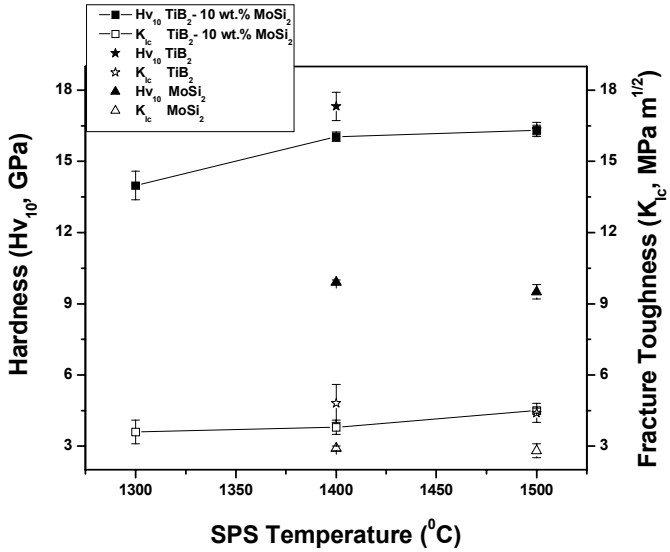

Fig. 4. Plot of Vickers Hardness (H_{v10}) and Fracture Toughness (according to Anstis et. al.,) against SPS temperature for TiB_2 -10 wt. % $MoSi_2$ composite and monolithic TiB_2 and $MoSi_2$ respectively.